Metallomics, 14, 2022, mfac008
https://doi.org/10.1093/mtomcs/mfac008
Advance access publication date: 12 February 2022
Paper

Rhenium–guanidine complex as photosensitizer: trigger HeLa cell apoptosis through death receptor-mediated, mitochondria-mediated, and cell cycle arrest pathways

Shu-Fen He[1,2,‡], Jia-Xin Liao[1,‡], Min-Ying Huang[1], Yu-Qing Zhang[1], Yi-Min Zou[1], Ci-Ling Wu[1], Wen-Yuan Lin[1], Jia-Xi Chen[1,*] and Jing Sun[1,*]

[1]School of Pharmacy, Guangdong Medical University, Dongguan 523808, China and [2]Department of Pharmacy, Dongguan People's Hospital, Dongguan, 523059, China

*Correspondence: Xincheng Road, Guangdong Medical University, Dongguang 523808, Guangdong, China. Tel.: +86-769-2289-6322; E-mail: jiaxi@gdmu.edu.cn (Jia-Xi Chen); sunjing@gdmu.edu.cn (Jing Sun).

‡Contributed equally to this work.

Abstract

The growing evidence over the past few decades has indicated that the photodynamic antitumor activity of transition metal complexes, and Re(I) compounds are potential candidates for photodynamic therapy. This study reports the synthesis, characterization, and anti-tumor activity of three new Re(I)–guadinium complexes. Cytotoxicity tests reveal that complex **Re1** increased cytotoxicity by 145-fold from $IC_{50} > 180\ \mu M$ in the dark to $1.3 \pm 0.7\ \mu M$ following 10 min of light irradiation (425 nm) in HeLa cells. Further, the mechanism by which **Re1** induces apoptosis in the presence or absence of light irradiation was investigated, and results indicate that cell death was caused through different pathways. Upon irradiation, **Re1** first accumulates on the cell membrane and interacts with death receptors to activate the extrinsic death receptor-mediated signaling pathway, and then is transported into the cell cytoplasm. Most of the intracellular **Re1** locates within mitochondria, improving the reactive oxygen species level, and decreasing mitochondrial membrane potential and ATP levels, and inducing the activation of caspase-9 and, thus, apoptosis. Subsequently, the residual **Re1** can translocate into the cell nucleus, and activates the p53 pathway, causing cell cycle arrest and eventually cell death.

Keywords: Re(I) complex, cytotoxicity, phototoxicity, membrane receptors, apoptosis, mechanism

Graphical abstract

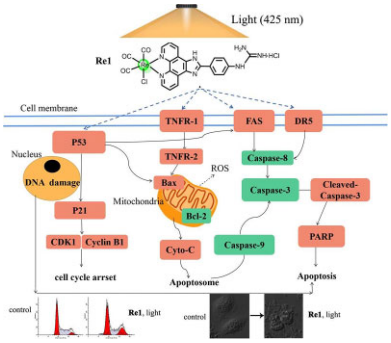

Rhenium complexes act as photosensitizer to induce apoptosis in HeLa cells.

Introduction

Despite the extensive progress in disease prevention by vaccines, screening, early detection, and treatment, cervical cancer remains the second most common cancer faced by women worldwide.[1–2] To date, the traditional treatments for cervical cancer include surgery, radiotherapy, and chemotherapy, but these are hindered by the disadvantages of strong invasion, poor targeting, and high recurrence rate.[3] Therefore, it is urgent to develop an efficient and safe cervical cancer treatment and drugs to enhance patients' survival rate and quality of life. Among these treatments, photodynamic therapy (PDT) has broad prospects, owing to lower trauma, less toxicity, and shorter time of the treatment.[4–6]

Compared with traditional photosensitizers (porphyrins, phthalocyanines, etc.) and material compounds, the phosphorescence properties of ruthenium,[7] iridium,[8] and rhenium[9] have attracted much research attention. Some of these compounds, such as TLD1433, have entered clinical trials.[10] Tricarbonyl Re(I)

Received: October 30, 2021. **Accepted:** January 27, 2022

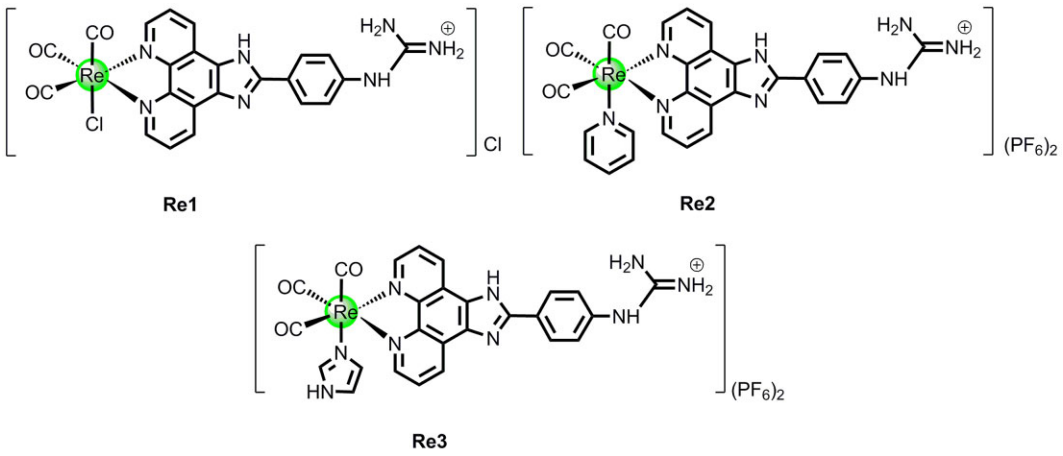

Fig. 1 Chemical structures of Re(I) complexes **Re1**–**Re3**.

is easy to modify and coordinate, and most Re(I) complexes have the potential to be used as cell imaging agents, anti-tumor drugs, and photosensitizers.[11–20] Previous studies report that mitochondria-targeted tricarbonyl Re(I) complexes lead to tumor cell death through irreversible oxidative stress and disruption of glutathione metabolism.[21] DNA photolysis studies show that Re–NLS and Re–Bomesin compounds can accumulate in the nucleus and significantly increase cytotoxicity under light irradiation, damaging DNA through singlet oxygen and thus leading to cell apoptosis.[22] Although the photophysical properties and anti-tumor mechanism of Re(I) complexes have been extensively explored, limited studies have investigated these complexes on the cellular level and in animals. Moreover, the mechanism of the photodynamic effect is still unclear.

It has been reported that the expression levels of cell membrane receptors in cancer cells and normal cells vary notably.[23] Based on this difference, the rational design of cancer-targeted drugs is a promising strategy. Death receptors (DRs), such as associated protein with death domain (FAS) and tumor necrosis factor (TNF) receptors, are membrane proteins of the TNF-R superfamily that are capable of inducing apoptosis and, thus, have attracted increasing research interest in the field of cancer research.[24–25] In literature, numerous works have reported that targeting receptors TNF-related apoptosis-inducing ligand (TRAIL), FAS, and TNF can selectively trigger apoptosis of cancer cells.[26–27] Therefore, exploring the mechanism of action between Re(I) complexes and the membrane receptor is significant for designing reasonably structured membrane receptor-targeted anti-cancer drugs.

Our previous studies have shown that some Ru(II) and Ir(III) metal complexes with guanidine exhibit good photodynamic therapeutic potential.[28–29] Under light irradiation, such compounds can be positioned in the mitochondria to activate apoptosis. Based on this, we synthesized and characterized three Re(I) complexes containing guanidinium groups as ligands, investigated their anticancer activity in the presence and absence of light irradiation, and elucidated the respective mechanisms (Fig. 1).

Results and discussion

Synthesis, characterization, and photophysical properties

Ligand L was synthesized by the methods we previously reported.[30] Complex **Re1** was prepared by mixing L and $Re(CO)_5Cl$ in methanol/toluene (1:1) and refluxed at 80°C under the protection of argon for 4 h in the dark. Crude products were purified by recrystallization with $CH_3CN/CH_3CH_2OCH_2CH_3$. Different monodentate ligands, namely pyridine (for **Re2**) and imidazole (for **Re3**), and **Re1** were refluxed in methanol or tetrahydrofuran under argon for 24 h to obtain complexes **Re2** and **Re3**. The chemical structures of the three complexes were completely characterized with mass spectrometry, ^{1}H NMR spectroscopy, and elemental analysis (Figs. S1–S6). Regarding the data of the mass spectrometry, ^{1}H NMR spectroscopy, and elemental analysis, it was verified the molecular structure of three complexes accord with theoretical values. The UV–Vis absorption spectra of complexes **Re1**–**Re3** in PBS, CH_3CN, and CH_2Cl_2 were also obtained using a UV–Vis spectrometer. The relatively strong absorption band at about 250–330 nm in the ultraviolet region can be attributed to ligand absorption ($\pi\rightarrow\pi^*$), while the relatively weak band at 380–430 nm can be ascribed to metal–ligand charge transfer absorption (Fig. S7).[31] Upon 405 nm excitation, these complexes showed yellow emission in PBS, CH_3CN, and CH_2Cl_2 at 298 K (Fig. S8). The photophysical properties of **Re1**–**Re3** are summarized in Table S1.

In vitro antitumor evaluation

The cytotoxicities and phototoxicity of complexes **Re1**–**Re3** and cisplatin were tested against several cancer cell lines (HeLa, HepG2, MCF-7, A549) and a non-tumorigenic LO2 cell line by the 3-(4,5-dimethylthiazol-2-yl)-2,5-diphenyltetrazolium bromide assay (Table 1 and Fig. S9). Accordingly, **Re2** and **Re3** had IC_{50} values ranging from 8.7 to 81.7 μM, thus showing moderate antitumor activity to cancer cells in the dark. Compared to cisplatin, all three Re(I) complexes displayed no obvious anti-tumor advantages but did demonstrate higher phototoxicity upon visible light irradiation (425 nm, 40 mW·cm^{-2}) under the same conditions. Notably, in HeLa cells, **Re1** had little cytotoxicity (IC_{50} = 185.4 μM) in the dark but displayed the highest phototoxicity index (PI) of >142. Regrettably, **Re1** did not show higher selectivity for the tested cancer cells compared to non-tumorigenic LO2 cells upon visible light irradiation. Due to its superior phototoxicity, **Re1** was chosen as the compound of interest for further mechanistic investigations.

Assessment of lipophilicity

The lipophilicities of the three complexes were examined with the flask-shaking method. The log*Po/w* values of **Re1**, **Re2**, and **Re3** were determined to be −0.95, −0.75, and −0.26, respectively

Table 1. Cytotoxicity ($IC_{50}/\mu M$) of the compounds in the absence and presence 425 nm light toward different cell lines

	IC_{50} (μM)									
	HeLa		HepG2		MCF-7		A549		LO2	
Complexes	Dark[a] (light[b])	PI[c]	Dark (light)	PI	Dark (light)	PI	Dark (light)	PI	Dark (light)	PI
Re1	185.4 ± 3.5 (1.3 ± 0.7)	142.6	19.5 ± 1.2 (4.7 ± 0.9)	4.1	29.8 ± 0.9 (5.1 ± 1.6)	5.8	45.0 ± 1.4 (4.0 ± 0.9)	11.3	61.3 ± 3.6 (2.7 ± 0.7)	22.7
Re2	81.3 ± 2.2 (12.0 ± 1.1)	6.8	38.5 ± 2.0 (7.3 ± 1.7)	5.3	45.6 ± 2.9 (9.9 ± 1.8)	4.6	49.9 ± 2.9 (9.5 ± 1.1)	5.3	53.5 ± 2.9 (9.0 ± 1.3)	5.9
Re3	34.4 ± 1.9 (0.9 ± 0.3)	38.2	8.7 ± 1.6 (0.7 ± 0.2)	12.4	36.1 ± 2.4 (1.6 ± 0.4)	22.6	27.2 ± 1.9 (0.9 ± 0.1)	30.2	39.2 ± 3.3 (1.6 ± 0.6)	24.5
Cisplatin	13.3 ± 1.6 (12.0 ± 0.7)	1.11	58.4 ± 2.4 (49.2 ± 0.8)	1.19	15.4 ± 3.2 (7.2 ± 1.4)	2.14	13.5 ± 1.7 (12.8 ± 0.4)	1.1	42.4 ± 3.0 (20.4 ± 1.0)	2.1

[a]Cells were incubated with the indicated complexes in the dark for 48 h. [b]Cells were incubated with the indicated complexes for 12 h in the dark and then irradiated with light at 425 nm. [c]PI = phototoxicity index, the ratio of the IC_{50} values in dark to those obtained upon light irradiation. Each value represents the mean ± SD of three independent experiments.

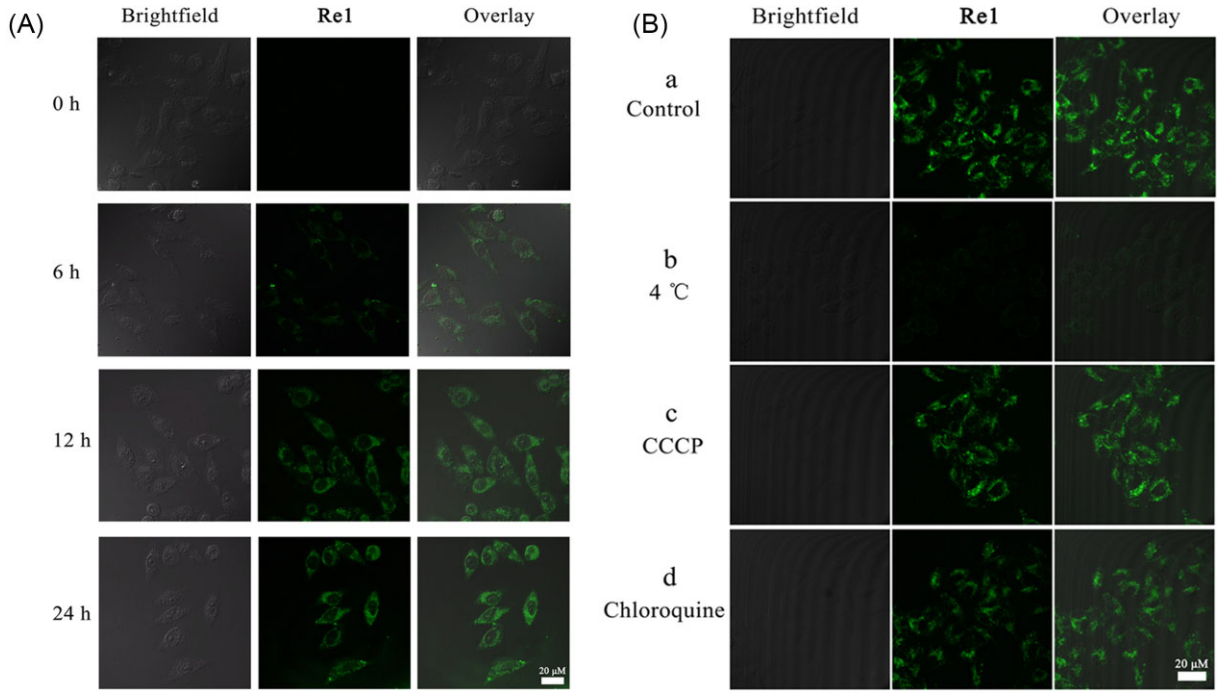

Fig. 2 (A) Confocal microscopy images of HeLa cells after 0, 12, and 24 h incubation with **Re1** (100 μM). (B) Confocal microscopy images of HeLa cells after incubation with **Re1** (100 μM) at indicated conditions: (a) HeLa cells were incubated with **Re1** at 37°C for 12 h; (b) HeLa cells were incubated with **Re1** at 4°C for 12 h; (c) HeLa cells were incubated with **Re1** at 37°C for 12 h after pre-incubation with 20 μM carbonyl cyanide metachlorophenylhydrazone at 37°C for 1 h; and (d) HeLa cells were incubated with **Re1** at 37°C for 12 h after pre-incubation with 50 μM chloroquine at 37°C for 1 h.

(Fig. S10). Many studies have indicated that structure and lipophilicity affect the cellular transportation, uptake, location, and action mechanisms of metal complexes, largely contributing to their anticancer activities.[32,33] Moreover, it was found that the lipophilicity of the three complexes follows the order: **Re3** > **Re2** > **Re1**, which is positively correlated with their toxicity to HeLa cells in the dark. As the least lipophilicity complex, **Re1** moved into the nucleus with light irradiation faster than the other complexes. This may be due to the increased energy of cells in the presence of light, which induced more **Re1** to cross the cell membrane into the cytoplasm. Therefore, **Re1** with lower lipophilicity may be more conducive to enter the nucleus. Likewise, Chao's group speculated that cationic metal complexes with lower lipophilicity may achieve nuclear absorption easier, as long as they can first penetrate through the plasma membrane of the cell.[34] In addition, due to the relatively lower lipophilicity, the complexes can selectively stain the cell plasma membrane, improving their probability of binding to death receptors on the cell membrane surface of tumor cells.[35–36]

Cellular uptake mechanism

As Re(I) complexes possess rich photophysical properties, we can monitor their transportation process into cancer cells and intracellular distribution conveniently. Figure 2 shows that **Re1** started to accumulate in the cytoplasm after 6 h then penetrated the

cytoplasm after 12 h of co-cultivation with HeLa cells in the dark, demonstrating green fluorescence (Fig. 2A).

As previously reported, the two main penetrating mechanisms related to the transport of small molecules across the cell membrane include energy-dependent endocytosis (e.g. endocytosis and active transport) and energy-independent direct penetration (e.g. facilitated diffusion and passive diffusion).[37–39] As presented in Fig. 2B, incubating HeLa cells with **Re1** at a lower temperature (4°C) resulted in a decrease in cellular uptake efficiency. However, the ability of **Re1** to cross the plasma membrane was not affected by the presence of the metabolic inhibitor carbonyl cyanide m-chlorophenyl hydrazone (CCCP) and the endocytosis regulator chloroquine. These results suggest that the uptake of **Re1** mainly occurs through an energy-dependent mechanism, which means that light may promote the ability of **Re1** to enter cells.

Induction of apoptosis

Re1-induced cell death and morphological changes were examined using Hoechst 33 342 staining and confocal microscopy. With the increase of concentration, the morphology of the **Re1**-treatment cells changed compared with the control cells in the dark and under light irradiation (Fig. 3A). After 24 h treatment with **Re1**, the cells exhibited typical apoptotic morphology, such as nuclear fragments, condensed chromatin, and apoptotic bodies.[40] Therefore, these findings demonstrate that **Re1** could induce apoptosis in HeLa cells. Subsequently, cellular apoptosis was assessed by a flow cytometry assay with PI/Annexin-V staining. Early and late apoptosis were progressively increased under different light conditions (Fig. 3B). Of these, **Re1** (100 μM) treatment increased the percentage of both early and late apoptosis to 3.90% and 29.2%, respectively, compared with the vehicle-treated cells (2.66% and 5.02%, respectively) in the dark. Moreover, **Re1** (10 μM) treatment also enhanced the percentage of early and late apoptosis by 1.87% + 83.7%, respectively, compared with the vehicle-treated cells (3.83% + 9.25%, respectively) under light irradiation. These data suggest that the ability of **Re1** to induce apoptosis in HeLa cells is stronger with light illumination.

Apoptosis is an intricate and precise process regulated by several relevant proteins, which can be classified into extrinsic (death ligand) and intrinsic (mitochondrial) pathways.[41] Caspases belonging to a family of cysteine proteases play important roles in the death of apoptotic cells in diverse biological systems.[42] In particular, caspase-3 is considered as a central modulator of apoptosis and is activated in both extrinsic and intrinsic pathways, which can be mediated by caspase-8 and -9 initiators, respectively.[43] To further clarify the latent mechanism of **Re1**, western blotting was performed to measure the expression levels of caspase-3, -8 and -9. As presented in Fig. 3C, **Re1** treatment without irradiation caused the dose-dependent activation of caspase-3 and remarkable elevation of cleaved caspase-3, while changes of caspase-8 and -9 expression levels in HeLa cells were negligible (Fig. 3C). However, after **Re1** treatment under light irradiation for 24 h, the expression levels of caspase-3, -8, and -9 were reduced significantly, whereas levels of cleaved caspase-3 increased remarkably (Fig. 3D). Taken together, these results demonstrate that **Re1** may trigger HeLa cell apoptosis through caspase-dependent extrinsic and intrinsic pathways under irradiation, which follows a different mechanism than that which occurs in dark conditions.

Membrane-targeted and activation of death receptors

To investigate whether **Re1** could induce apoptosis through the death receptor pathway, the co-staining of **Re1** and cell membrane red fluorescent dye (DiD) was used to study localization upon exposure to irradiation of 425 nm. The results showed that **Re1** accumulated in a time-dependent manner in HeLa cells. During the initial 4 h, the green fluorescence of **Re1** gradually overlapped with the red fluorescence of DiD, indicating that **Re1** is mainly concentrated on the membrane, and the complex could have a sufficient interaction with the membrane receptors. Then, most of **Re1** crossed the membrane and accumulated in the cytoplasm in 8 h and was finally enriched in the cells at 12 h. Until 24 h later, an increasing amount of **Re1** was observed in the nucleus accompanied by a reduction in the cell membrane (Fig. 4A). Furthermore, the expression levels of several death receptor-related proteins in HeLa cells were examined. As showed in Fig. 4B, cell treatment with **Re1** under light caused an outstanding dose-dependent increase in the expressions of TNFR-1, TNFR-2, FAS, and DR5 (Fig. 4C), while only invisible change was observed in the expression of these proteins in the dark (Fig. 4B). These results indicated that **Re1**-induced apoptosis under light irradiation was mediated via the extrinsic death receptor pathway.

Cytoplasm localization under the light irradiations

To further understand the mechanism by which **Re1** enters the cytoplasm under light irradiation of 425 nm, its subcellular localization was further evaluated in HeLa cells by fluorescence microscopy coupled with a fluorescent probe. Considering **Re1** mainly aggregated in the cytoplasm after co-incubation with cells for 8 h, we explored the localization of the complex during this period. As shown in Fig. 5A, **Re1** demonstrated a high degree of co-localization with the organelle-specific stain MitoTracker® Red CMXRos (MTR), with a Pearson co-localization coefficient (PCC) of 0.89. Under the same conditions, the PCC between **Re1** and Lysotracker Red (LTR) was only 0.48. These results confirm that **Re1** spent most of the time in mitochondria after entering the cytoplasm. Further studies are required to confirm whether or not **Re1** is able to induce apoptosis of HeLa cells via a mitochondrial-dependent pathway. Therefore, the expressions of Bcl-2, Bax, Cyto-c, and PARP, which are typical apoptotic proteins of the mitochondrial apoptosis pathway, were detected using western blot analysis. As presented in Fig. 5B and C, under light conditions, the expressions of Bax, Cyto-c and PARP were up-regulated with increasing concentrations of **Re1**, while **Re1** down-regulated the expression levels of Bcl-2. Besides, similar results were observed under dark conditions, except for the PARP protein, whose expression level had no obvious change. Together, these results suggest that **Re1**-induced apoptosis under light irradiation via endogenous pathways involving mitochondria.

Apoptosis-related mitochondrial events

As a mediator of apoptosis, reactive oxygen species (ROS) can trigger a range of mitochondria-related events, such as apoptosis and the decline of mitochondrial membrane potential (MMP).[44–46] What is more, induction of apoptosis by PDT is thought to occur through the production of intracellular ROS.[47] Hence, it is significant to investigate the ability of **Re1** to stimulate ROS generation and accumulation for elucidating the potential mechanism of apoptosis. In this work, ROS levels were measured via

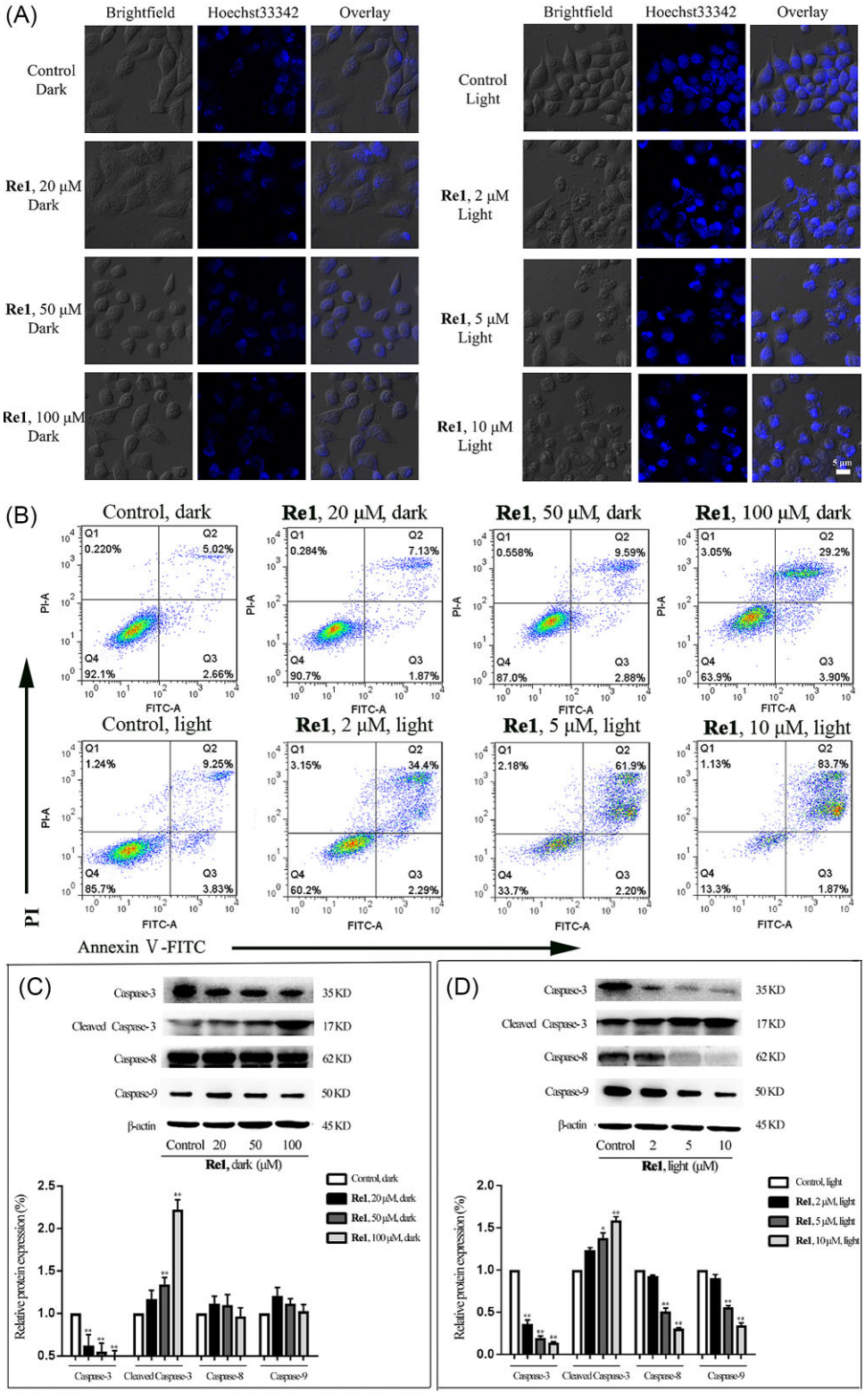

Fig. 3 (A) Hoechst 33 342 stained HeLa cells after treatment of **Re1** at the indicated concentrations for 24 h. (B) Flow cytometric quantification of Annexin V and PI double labeled HeLa cells after treatment with **Re1** for 24 h. (C) Western blot analysis of **Re1** on the expression of caspase-3, cleaved caspase-3, caspase-8, and caspase-9. HeLa cells were incubated with indicated concentrations of **Re1** for 24 h in the dark. (D) The same treatment as (B) under light irradiation. Photoirradiation (425 nm, 40 mW·cm^{-2}, 10 min) was performed after the cells were incubated with **Re1** for 30 min. ($^{*}P < 0.05$, $^{**}P < 0.01$).

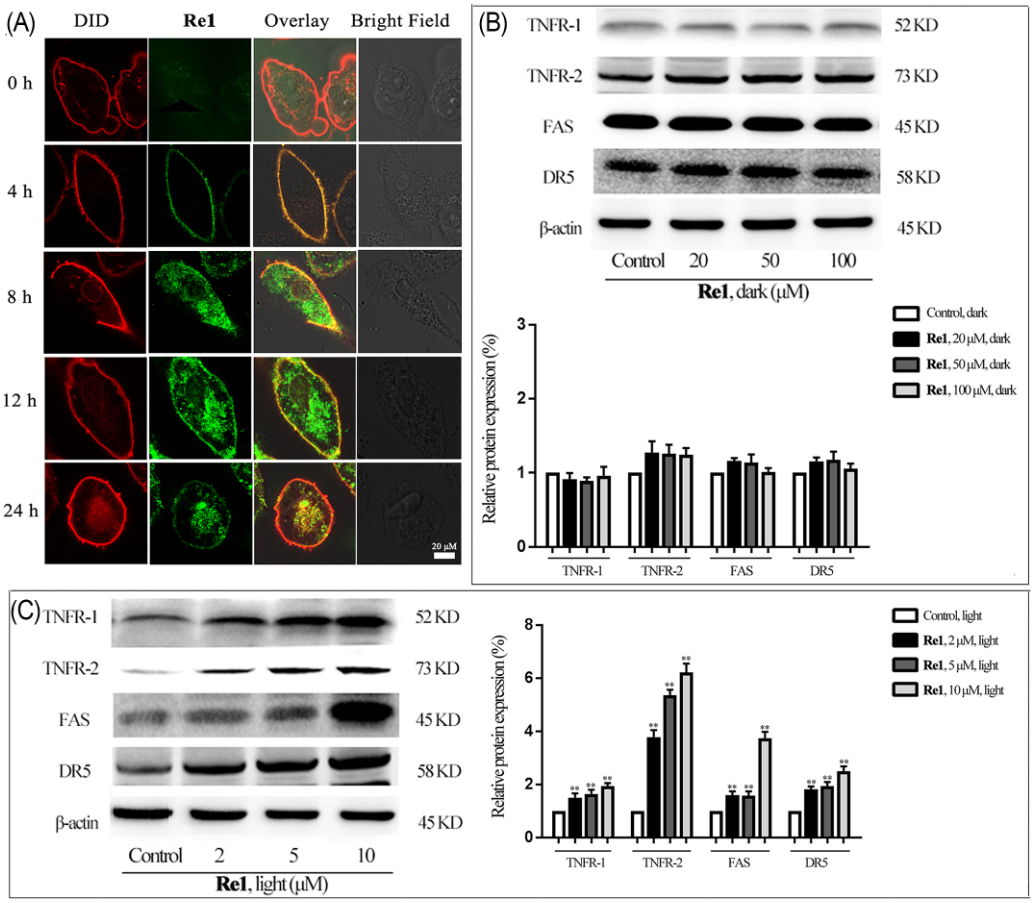

Fig. 4 (A) Confocal microscopy images of HeLa cells incubated with **Re1** (5 μM) and red fluorescent dye (DiD; 5 μM, 0.5 h) at 37°C for 0, 4, 8, 12, and 24 h. **Re1** was excited at 405 nm and DiD was excited at 552 nm. (B) Western blot analysis of **Re1** on the expression of TNFR-1, TNFR-2, FAS, and death receptor 5. HeLa cells were incubated with indicated concentrations of **Re1** for 24 h, in the dark. (C) The same treatment as (B), under light irradiation. Photoirradiation (425 nm, 40 mW·cm^{-2}, 10 min) was performed after the cells were incubated with **Re1** for 30 min. ($^{*}P < 0.05$, $^{**}P < 0.01$).

2′,7′-dichlorodihydrofluorescein diacetate (DCFH-DA) fluorescence. Results show that the fluorescence intensity in HeLa cells increased in a concentration-dependent manner after treatment with **Re1** both in the absence and presence of light (Fig. 6A). Moreover, the cellular ROS levels were examined by flow cytometry. After 12 h of co-incubation with **Re1** (100 μM in the dark and 10 μM under illumination at 425 nm), the mean 2′,7′-dichlorofluorescein (DCF) green fluorescence intensity increased to approximately 2.9-fold and 5.6-fold higher than the control groups (Fig. 6B). Furthermore, HeLa cells were pretreated with N-acetylcysteine, an ROS scavenger, to further verify the effect of ROS on cell death. As shown in Fig. S11, after pre-incubating with N-acetylcysteine, the cell viability of **Re1**-treated cells increased from 90.9 ± 2.6% to 92.8 ± 5.0% (**Re1**, 20 μM), 87.9 ± 5.7% ± to 91.2 ± 7.3% (**Re1**, 50 μM), and 83.5 ± 3.1% to 90.9 ± 2.2% (**Re1**, 100 μM) in the dark and from 63.1 ± 5.6% to 82.2 ± 7.6% (**Re1**, 2 μM), 33.7 ± 4.0% to 59.0 ± 5.8% (**Re1**, 5 μM), and 15.3 ± 2.9% to 34.8 ± 3.3% (**Re1**, 10 μM) under the light conditions, respectively. All these data demonstrate that **Re1** can induce ROS generation under different light conditions.

Disruption of MMP is a landmark event of cellular apoptosis.[48–50] When MMP decreases, JC-1 fluorescence is displayed as green monomers, while higher MMP correlates to red JC-1 aggregates, indicating normal mitochondria. After treatment with **Re1** for 12 h (in the dark and under light irradiation), HeLa cells exhibited a reduction in red fluorescence and increase in green fluorescence (Fig. 6C). Similar results were recorded by flow cytometry. As depicted in Fig. 6D, the red/green fluorescence intensity ratio decreased in a concentration-dependent manner in the dark (control: 79.0 ± 1.9; 20 μM **Re1**: 72.1 ± 1.7; 50 μM **Re1**: 51.2 ± 2.8; 100 μM **Re1**: 37.5 ± 3.4) and light conditions (control: 81.6 ± 3.2; 2 μM **Re1**: 52.3 ± 3.7; 5 μM **Re1**: 34.7 ± 2.3; 10 μM **Re1**: 10.0 ± 1.3). This result indicates that lower concentrations of **Re1** under light irradiation could impair the mitochondrial integrity.

Since mitochondria are regarded as the energy factory of cells in which ATP is created, mitochondrial dysfunction is accompanied by reduced ATP.[51–53] After **Re1** treatment, ATP levels in HeLa cells were reduced to 68.1% (2 μM), 37.3% (5 μM), and 8.3% (10 μM) under light irradiation compared to the control. However, the results obtained in the dark were not notably altered versus control, confirming that **Re1** can affect mitochondrial integrity under light conditions.

Nucleus entry and cell cycle arrest

In the cell membrane DiD staining experiment, after light irradiation, **Re1** entered the nucleus at 24 h, which was confirmed by Hoechst 33342. As shown in Fig. 7A, the green fluorescence of **Re1** closely overlaps with the blue fluorescence representing cell nuclei. It is well known that genetic information and encodes proteins are contained in the cell nucleus, which

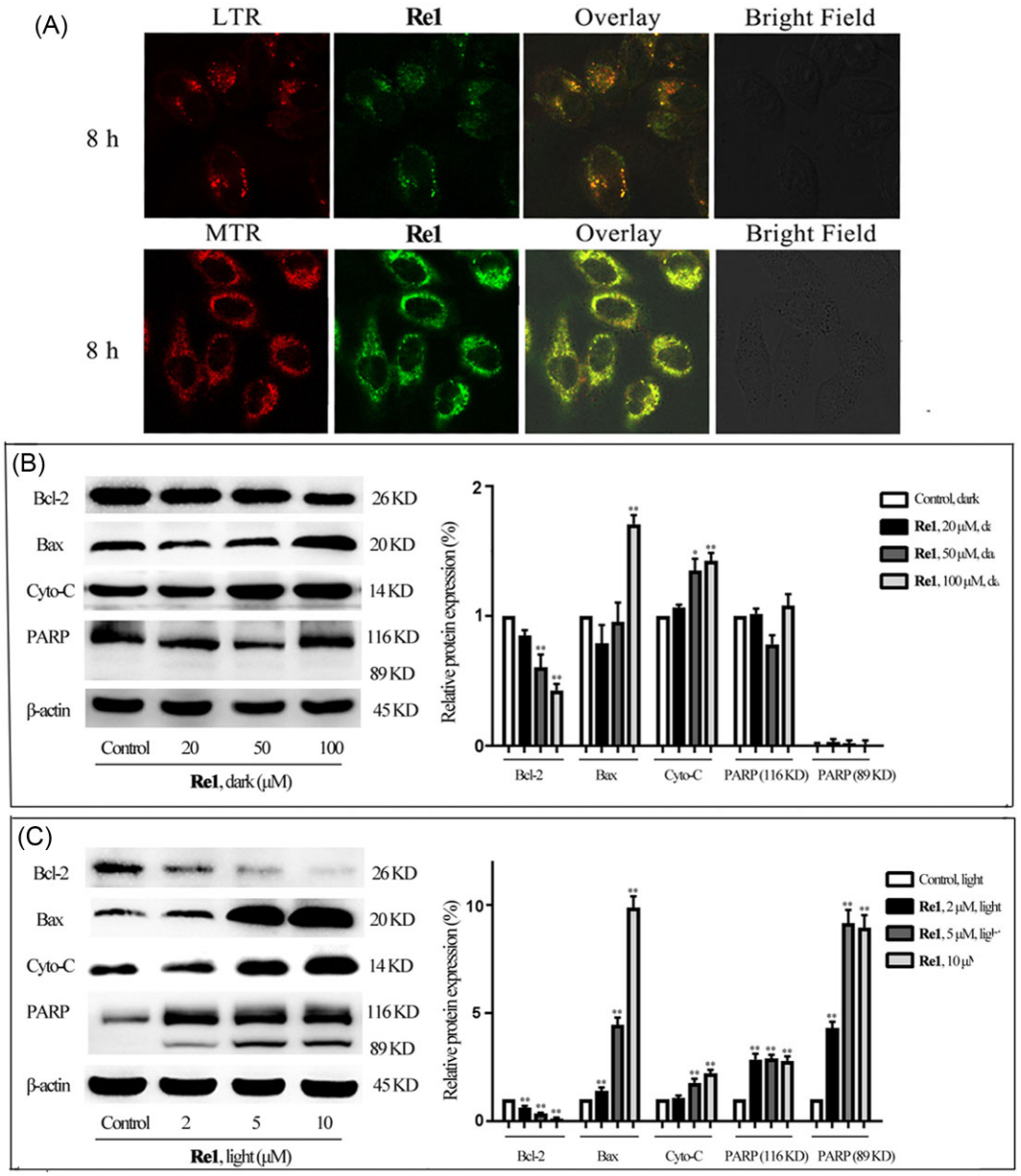

Fig. 5 (A) Confocal microscopic images of HeLa cells incubated with **Re1** (5 μM, 8 h), MitoTracker® Red CMXRos (MTR; 100 nM, 0.5 h) and Lyso-tracker Red (LTR; 100 nM, 0.5 h). **Re1** excitation at 405 nm, and MTR and LTR excitation at 552 nm. (B) Western blot analysis of **Re1** on the expression of Bcl-2, Bax, Cyto-c, PARP. HeLa cells were incubated with indicated concentrations of **Re1** for 24 h in the dark. (C) The same treatment as (B) under light irradiation. Photoirradiation (425 nm, 40 mW·cm^{-2}, 10 min) was performed after the cells were incubated with **Re1** for 30 min. ($^{*}P < 0.05$, $^{**}P < 0.01$).

governs the mechanisms of cell proliferation, differentiation, and function.[54–55] Numerous studies have revealed that cell proliferation is a cell cycle–dependent process in cancer development, and thus many antitumor drugs are designed based on this mechanism to combat cancer.[56–58] Compared with the control group, **Re1** showed a negligible effect on the cell cycle in dark conditions, while the combination of **Re1** and light arrested the cell cycle in the G2/M phase in a concentration-dependent manner (Fig. 7B). Following a 24 h treatment with **Re1** (10 μM), the percentages of cells were reduced at the G0/G1 (Control: 49.4 ± 1.3%; **Re1**: 35.2 ± 1.0%) and S phases (control: 43.2 ± 1.8; **Re1**: 25.7% ± 1.8), while there was an accumulation in the G2/M phase (control: 7.4% ± 2.0; **Re1**: 32.1% ± 2.3) (Table S2 and Fig. S12).

In addition, the equilibrium between cell proliferation and differentiation is reflected in the appearance of the nucleus and is controlled by the balance established among expressed proteins. To elucidate the effect of **Re1** with PDT treatment on the cell cycle and cell apoptosis, the expressions of p53, p21, cyclin-dependent kinases (CDK)1, and Cyclin B1 protein were analyzed by western blot. As a cell cycle checkpoint, and a vital downstream effector of p53, p21 mediates the inactivation of various cyclin–CDK complexes.[59] Under the light, **Re1** simultaneously activated p53 and p21 and significantly down-regulated CDK1 and Cyclin B1, which are two key factors of G2/M phase arrest[60–62] (Fig. 7D). No apparent changes to CDK1 and Cyclin B1 were observed in the dark, while the expression levels of p53 and p21 were up-regulated (Fig. 7C). These findings prove that **Re1** could trigger G2/M cycle arrest to further induce apoptosis via regulating the expression of related proteins, namely p53, p21, CDK1, and Cyclin B1, under light irradiation.

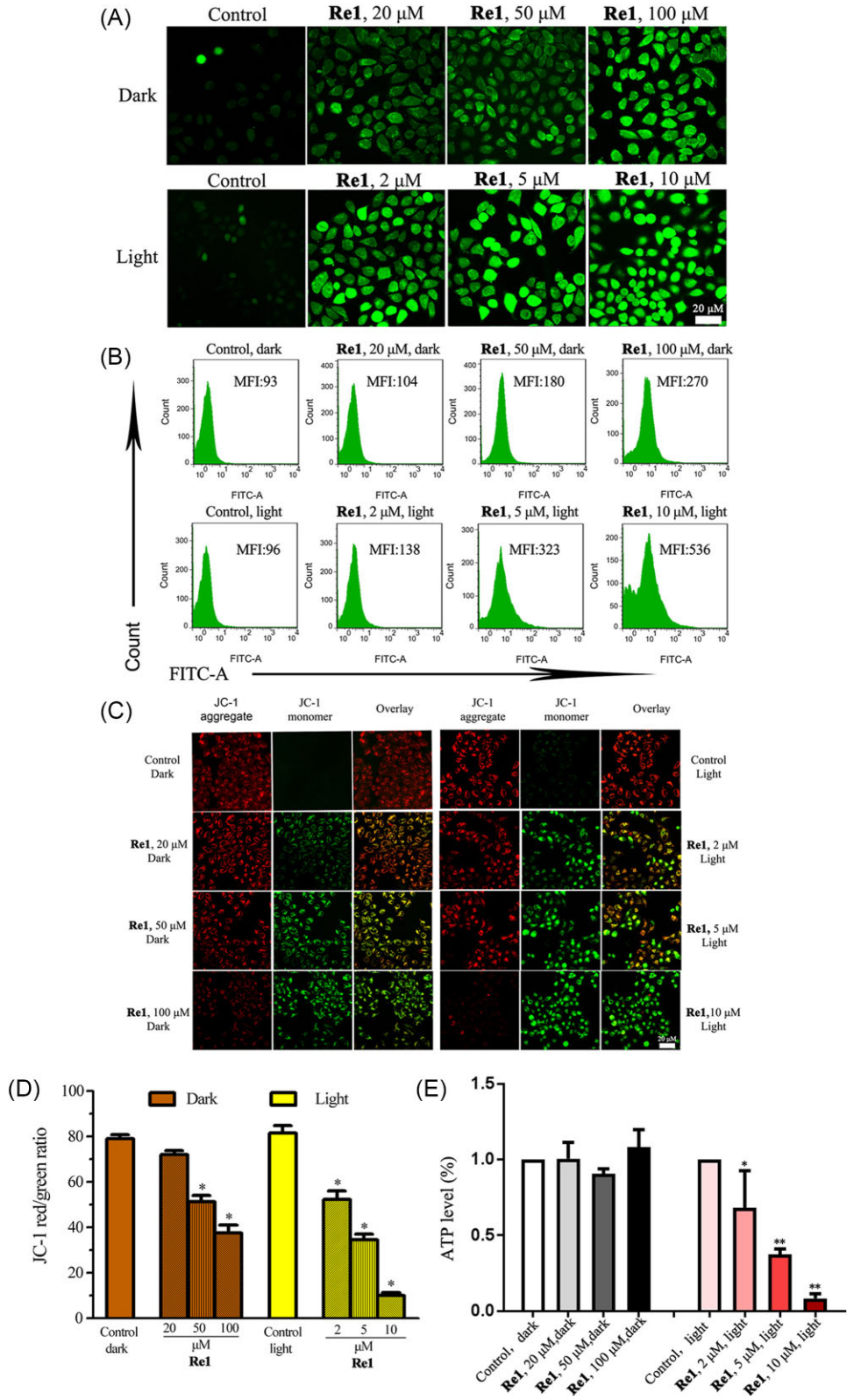

Fig. 6 Effects of **Re1** on reactive oxygen species (ROS) production. HeLa cells were incubated with **Re1** and labeled with DCFH-DA, then analyzed using confocal microscopy (A) and flow cytometry (B). Effects of **Re1** on mitochondrial integrity: (C) Fluorescence imaging of JC-1 labeled cells via confocal microscopy; (D) Effects of **Re1** on mitochondrial membrane potential (MMP) analyzed by JC-1 staining and flow cytometry. HeLa cells were treated with **Re1** at the indicated concentrations for 12 h. JC-1 was excited at 488 nm. (E) Intracellular ATP levels in HeLa cells after incubating with **Re1** at different concentrations. The light group of (A)-(E): Photoirradiation (425 nm, 40 mW·cm^{-2}, 10 min) was performed after the cells were incubated with **Re1** for 30 min. (*$P < 0.05$, **$P < 0.01$)

.

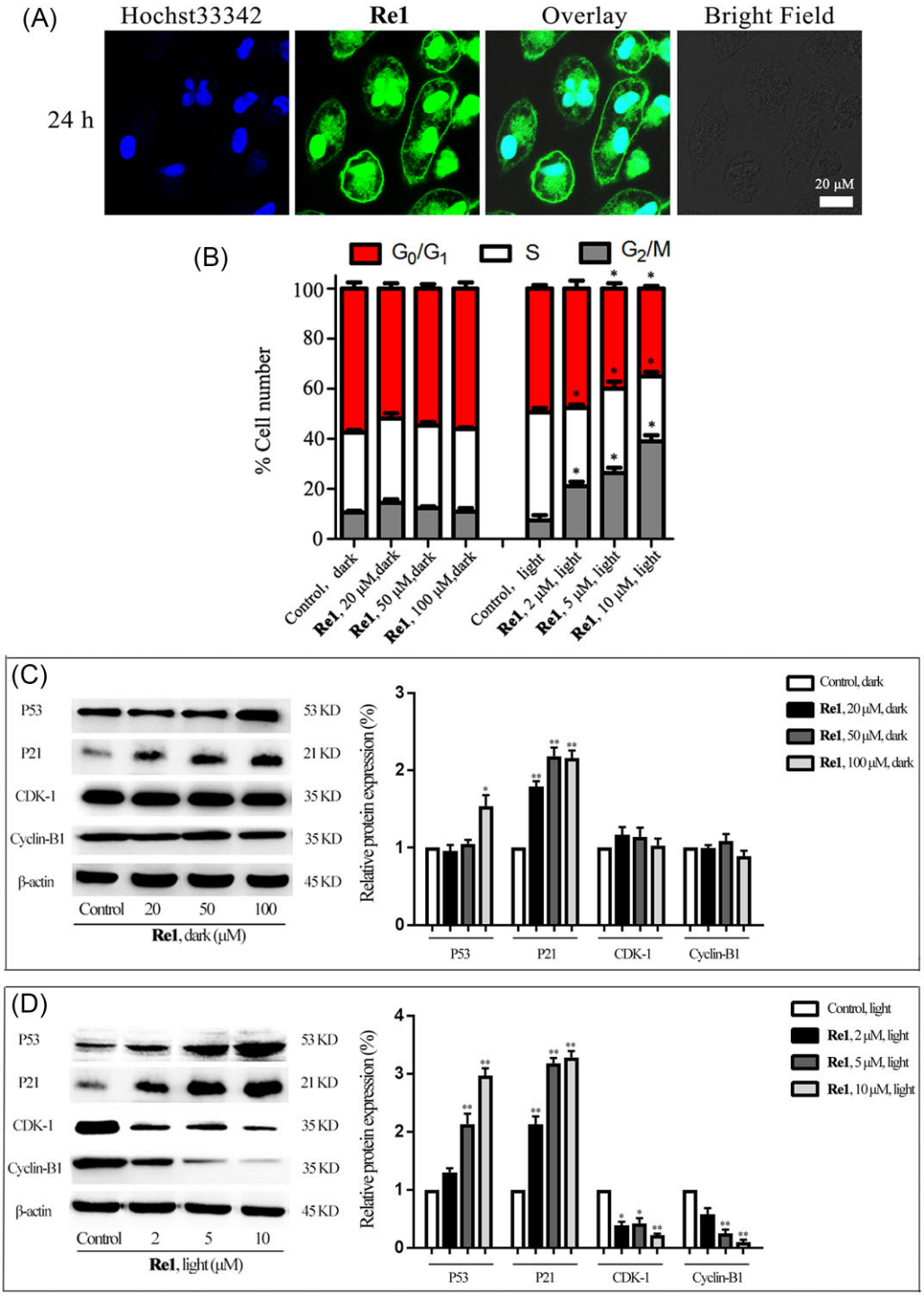

Fig. 7 (A) Co-localization of **Re1** (5 μM, 24 h) and Hoechst 33 342 dye in HeLa cells. (B) Effects of **Re1** on the distribution of HeLa cells in cell cycle population at indicated conditions for 24 h treatment. (*$P < 0.05$) (C) Western blot analysis of **Re1** on the expression of P53, P21, CDK1, Cyclin B1. HeLa cells were incubated with indicated concentrations of **Re1** for 24 h, in the dark. (D) The same treatment as (B), under light irradiation. Photoirradiation (425 nm, 40 mW·cm^{-2}, 10 min) was performed after the cells were incubated with **Re1** for 30 min.

Effect on cell migration

The ability to inhibit cell migration is an important marker for the antitumor activity of agents.[63–65] To assess the effect of **Re1** on cell migration, a cell scratch experiment was conducted. After treating with **Re1** at different concentrations for 24 and 48 h under dark conditions, the distance between the scratches was significantly lower. Comparatively, HeLa cells treated with **Re1** under light irradiation exhibited a significantly time- and concentration-dependent inhibition of wound healing integrity compared to the control group (Fig. 8).

Conclusions

In this study, three new rhenium–guanidine complexes were synthesized and characterized. The results display that complex **Re1** has great potential as a photosensitizer based on the various

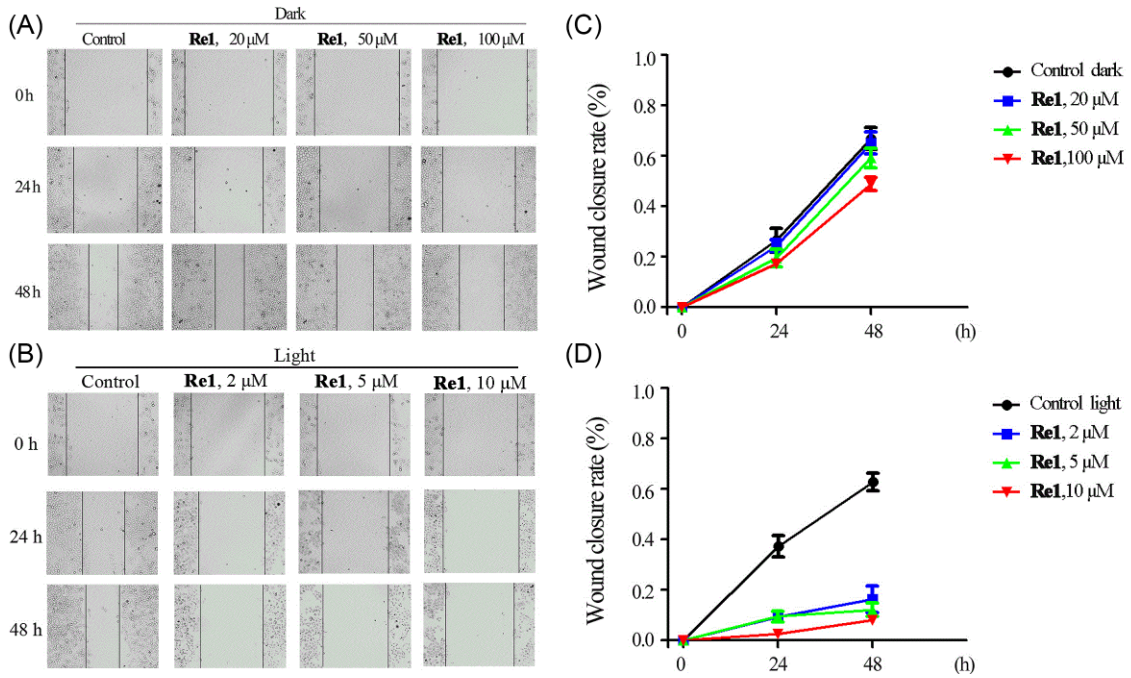

Fig. 8 Wound healing assay performed on HeLa cells. (A) The cells were incubated with **Re1** (20, 50, and 100 μM) for 0, 24, and 48 h in the dark. (B) The cells were incubated with **Re1** (2, 5, and 10 μM) for 0, 24, and 48 h. Photoirradiation (425 nm, 40 mW·cm^{-2}, 10 min) was performed after the cells were incubated with **Re1** for 30 min. Statistical data of wound healing assay of (C) dark and (D) light. (Wound closure (%) = [1 − (distance at indicated time)/(distance at 0 h)] × 100%).[64]

mechanisms by which it induces apoptosis both in the absence and presence of light. Specifically, in the dark, **Re1** is mainly distributed in the cytoplasm and triggers apoptosis by ROS elevation, reduction of ATP production, and loss of MMP at relatively high concentrations. Interestingly, **Re1** induces apoptosis through three pathways under light irradiation of 425 nm, including death receptor-mediated, mitochondria-mediated, and cell cycle arrest in HeLa cells. Further experiments demonstrated that **Re1** accumulated on the cell membrane during the first 4 h and promoted the activation of death receptors, leading to the extrinsic apoptotic pathway through caspase-8 activation. After **Re1** entered the cytoplasm and predominantly localized within the mitochondria, ROS production improved, cellular MMP and ATP levels decreased, and caspase-9 and its downstream protein were activated, causing cells to undergo mitochondrial apoptosis. Eventually, **Re1** translocated into the nucleus, activating the p53 signaling pathway and inducing cell cycle arrest in the G2/M phases to aggravate cellular apoptosis. Based on the results, this study reveals that **Re1** has great potential to be developed as a novel photosensitizer, which provides fundamental information for further advancements of PDT drugs for cervical cancer.

Supplementary material

Supplementary data are available at *Metallomics* online.

Funding

This work was supported by the National Natural Science Foundation of China (21101034), the Discipline Construction Project of Guangdong Medical University (4SG21004G), the Key Scientific Research Projects of Colleges and Universities in Guangdong Province (2020ZDZX2031), Dongguan Science and Technology of Social Development Program (20211800905082, 20211800905242), and the Project of Scientific Research Development Fund of Dongguan People's Hospital (K202015).

Conflicts of interest

The authors declare no competing financial interests.

Data availability

The data underlying this article are available in the article and in its online supplementary material.

References

1. C. L. Creutzberg, K. H. Lu and G. F. Fleming, Uterine cancer: adjuvant therapy and management of metastatic disease, *J. Clin. Oncol.*, 2019, 37, 2490–2500.
2. M. S. Zaman, N. Chauhan, M. M. Yallapu, R. K. Gara and S. C. Chauhan, Curcumin nanoformulation for cervical cancer treatment, *Sci. Rep.*, 2016, 6, 20051–20064.
3. J. H. Ha and Y. J. Kim, Photodynamic and cold atmospheric plasma combination therapy using polymeric nanoparticles for the synergistic treatment of cervical cancer, *Int. J. Mol. Sci.*, 2021, 22, 1172–1190.
4. V. N. Nguyen, Y. Yan, J. Zhao and J. Yoon, Heavy-atom-free photosensitizers: from molecular design to applications in the photodynamic therapy of cancer, *Acc. Chem. Res.*, 2020, 54, 207–220.
5. G. Li, D. Zhu, X. Wang, Z. Su and M. R. Bryce, Dinuclear metal complexes: multifunctional properties and applications, *Chem. Soc. Rev.*, 2020, 49, 765–838.
6. J. Karges, U. Basu, O. Blacque, H. Chao and G. Gasser, Polymeric encapsulation of novel homoleptic bis(dipyrrinato) zinc(II) complexes with long lifetimes for applications as photodynamic

therapy photosensitisers, *Angew. Chem. Int. Ed. Engl.*, 2019, 58, 14334–14340.
7. G. L. He, N. Xu, H. Y. Ge, Y. Lu, R. Wang, H. X. Wang, J. J. Du, J. L. Fan, W. Sun and X. J. Peng, Red-light-responsive Ru complex photosensitizer for lysosome localization photodynamic therapy, *ACS Appl. Mater. Inter.*, 2021, 13, 19572–19580.
8. Y. Q, Wu, J. Wu and W. Y. Wong, A new near-infrared phosphorescent iridium(III) complex conjugated to a xanthene dye for mitochondria-targeted photodynamic therapy, *Biomater. Sci.*, 2021, 14, 4843–4853.
9. A. M. H. Yip, J. Shum, H. W. Liu, H. Zhou, M. Jia, N. Niu, Y. Li, C. Yu and K. W. Lo, Luminescent rhenium(I)-polypyridine complexes appended with a perylene diimide or benzoperylene monoimide moiety: photophysics, intracellular sensing, and photocytotoxic activity, *Chem. Eur. J.*, 2019, 25, 8970–8974.
10. S. Monro, K. L. Colón, H. Yin, J. Roque, P. Konda, S. Gujar, R. P. Thummel, L. Lilge, C. G. Cameron and S. A. McFarland, Transition metal complexes and photodynamic therapy from a tumor-centered approach: challenges, opportunities, and highlights from the development of TLD1433, *Chem. Rev.*, 2019, 119, 797–828.
11. A. M. Ranieri, M. Vezzelli, K. G. Leslie, S. Huang, S. Stagni, D. Jacquemin, H. Jiang, A. Hubbsrd, L. Rigamonti, E. L. J. and Watkin, Structure illumination microscopy imaging of lipid vesicles in live bacteria with naphthalimide-appended organometallic complexes, *Analyst*, 2021, 146, 3818–3822.
12. Z. Y. Pan, D. H. Cai and L. He, Dinuclear phosphorescent rhenium(I) complexes as potential anticancer and photodynamic therapy agents, *Dalton Trans.*, 2020, 49, 11583–11590.
13. H. S. Liew, C. W. Mai, M. Zulkefeli, T. Madheswaran, L. V. Kiew, N. Delsuc and M. L. Low, Recent emergence of rhenium(I) tricarbonyl complexes as photosensitisers for cancer therapy, *Molecules*, 2020, 25, 4176–4198.
14. E. B. Bauer, A. A. Haase, R. M. Reich, D. C. Crans and F. E. Kühn, Organometallic and coordination rhenium compounds and their potential in cancer therapy, *Coordin. Chem. Rev.*, 2019, 393, 79–117.
15. A. Leonidova and G. Gasser, Underestimated potential of organometallic rhenium complexes as anticancer agents, *ACS Chem. Biol.*, 2014, 9, 2180–2193.
16. L. C. C. Lee, K. K. Leung and K. K. W. Lo, Recent development of luminescent rhenium(I) tricarbonyl polypyridine complexes as cellular imaging reagents, anticancer drugs, and antibacterial agents, *Dalton Trans.*, 2017, 46, 16357–16380.
17. C. C. Konkankit, S. C. Marker, K. M. Knopf and J. J. Wilson, Anticancer activity of complexes of the third row transition metals, rhenium, osmium, and iridium, *Dalton Trans.*, 2018, 47, 9934–9974.
18. K. Wähler, A. Ludewig, P. Szabo, K. Harms and E. Meggers, Rhenium complexes with red-light-induced anticancer activity, *Eur. J. Inorg. Chem.*, 807–811.
19. A. Kastl, S. Dieckmann, K. Wähler, T. Völker, L. Kastl, A. L. Merkel, A. Vultur, B. Shannan, K. Harms, M. Ocker, W. Parak, M. Herlyn and E. Meggers, Rhenium complexes with visible-light-induced anticancer activity, *ChemMedChem*, 2014, 8 (2013) 924–927.
20. S. C. Marker, S. N. MacMillan, W. R. Zipfel, Z. Li, P. C. Ford and J. J. Wilson, Photoactivated in vitro anticancer activity of rhenium(I) tricarbonyl complexes bearing water-soluble phosphines, *Inorg. Chem.*, 2018, 57, 1311–1331.
21. F. X. Wang, J. H. Liang, H. Zhang, Z. H. Wang, Q. Wan, C. P. Tan, L. N. Ji and Z. W. Mao, Mitochondria-accumulating rhenium(I) tricarbonyl complexes induce cell death via irreversible oxidative stress and glutathione metabolism disturbance, *ACS Appl. Mater. Inter.*, 2019, 11, 13123–13133.
22. A. Leonidova, V. Pierroz, R. Rubbiani, J. Heier, S. Ferrari and G. Gasser, Towards cancer cell-specific phototoxic organometallic rhenium(I) complexes, *Dalton Trans.*, 2014, 43, 4287–4294.
23. S. Plenchette, S. Romagny, V. Laurens and A. Bettaieb, S-nitrosylation in TNF superfamily signaling pathway: implication in cancer, *Redox Biol.*, 2015, 6, 507–515.
24. G. P. Amarante-Mendes and T. S. Griffifith, Therapeutic applications of TRAIL receptor agonists in cancer and beyond, *Pharmacol. Therapeut.*, 2015, 155, 117–131.
25. S. Prasad, J. H. Kim, S. C. Gupta and B. B. Aggarwal, Targeting death receptors for TRAIL by agents designed by Mother Nature, *Trends Pharmacol. Sci.*, 2014, 35, 520–536.
26. J. Gerspach, K. Pfizenmaier and H. Wajan, Therapeutic targeting of CD95 and the TRAIL death receptors, *Recent Pat. Anti-Canc.*, 2011, 6, 294–310.
27. O. Micheau, S. Shirley and F. Dufour. Br. J, Death receptors as targets in cancer, *Pharmacology*, 2013, 169, 1723–1744.
28. X. D. Song, B. B. Chen, S. F. He, N. L. Pan, J. X. Liao, J. X. Chen, G. H. Wang and J. Sun, Guanidine-modified cyclometalated iridium(III) complexes for mitochondria-targeted imaging and photodynamic therapy, *Eur. J. Med. Chem.*, 2019, 179, 26–37.
29. W. X. Chen, X. D. Song, S. F. He, J. Sun, J. X. Chen, T. Wu and Z. W. Mao, Ru(II) complexes bearing guanidinium ligands as potent anticancer agents, *J. Inorg. Biochem.*, 2016, 164, 91–98.
30. W. X. Chen, X. D. Song, J. X. Chen, X. H. Zhao, J. H. Xing, J. R. Ren, T. Wu and J. Sun, Synthesis, characterization, and DNA binding studies of two Ru(II) complexes containing guanidinium ligands, *Polyhedron*, 2016, 110, 274–281.
31. K. K. Lo, Luminescent rhenium(I) and iridium(III) polypyridine complexes as biological probes, imaging reagents, and photocytotoxic agents, *Acc. Chem. Res.*, 2015, 48, 2985–2995.
32. V. Pierroz, T. Joshi, A. Leonidova, C. Mari, J. Schur, I. Ott, L. Spiccia, S. Ferrari and G. Gasser, Molecular and cellular characterization of the biological effects of ruthenium(II) complexes incorporating 2-pyridyl-2-pyrimidine-4-carboxylic acid, *J. Am. Chem. Soc.*, 2012, 134, 20376–20387.
33. R. R. Ye, C. P. Tan, Y. N. Lin, L. N. Ji and Z. W. Mao, A phosphorescent rhenium(i) histone deacetylase inhibitor: mitochondrial targeting and paraptosis induction, *Chem. Commun.*, 2015, 51, 8353–8356.
34. X. J. Chao, M. Tang, R. Huang, C. H. Huang, J. Shao, Z. Y. Yan and B. Z. Zhu, Targeted live-cell nuclear delivery of the DNA 'light-switching' Ru(II) complex via ion-pairing with chlorophenolate counter-anions: the critical role of binding stability and lipophilicity of the ion-pairing complexes, *Nucleic Acids Res.*, 2019, 47, 10520–10528.
35. N. Zhao, Y. Li, W. Yin, J. B. Zhuang, Q. Jia, Z. L. Wang and N. Li, Controllable coumarin-Based NIR fluorophores: selective subcellular imaging, cell membrane potential indication, and enhanced photodynamic therapy, *ACS. Appl. Mater. Inter.*, 2020, 12, 2076–2086.
36. K. Li, Y. F. Lyu, Y. Huang, S. Xu, H. W. Liu, L. L. Chen, T. B. Ren, M. Y. Xiong, S. Y. Huan, L. Yuan, X. B. Zhang and W. H. Tan, A de novo strategy to develop NIR precipitating fluorochrome for long-term in situ cell membrane bioimaging, *P. Natl. Acad. Sci. U.S.A.*, 2021, 118, e2018033118.
37. A. Mishra and S. Batra, Thiourea and guanidine derivatives as antimalarial and antimicrobial agents, *Curr. Top. Med. Chem.*, 2013, 13, 2011–2025.
38. R. R. Ye, C. P. Tan, Y. N. Lin, L. N. Ji and Z. W. Mao, A phosphorescent rhenium(I) histone deacetylase inhibitor: mitochondrial target-

ing and paraptosis induction, *Chem. Commun.*, 51 (39), 8353–8356.
39. K. M. Knopf, B. L. Murphy, S. N. MacMillan, J. M. Baskin, M. P. Barr, E. Boros and J. J. Wilson, In vitro anticancer activity and in vivo biodistribution of rhenium(I) tricarbonyl aqua complexes, *J. Am. Chem. Soc.*, 2017, 139, 14302–14314.
40. H. F. Zhou, Y. He, J. Q. Zhu, X. J. Lin, J. Chen, C. Y. Shao, H. Y. Wan and J. H. Yang, Guhong injection protects against apoptosis in cerebral ischemia by maintaining cerebral microvasculature and mitochondrial integrity through the PI3K/AKT pathway, *Front. Pharmacol.*, 2021, 12, 650983–650999.
41. Y. Y. Tu, L. F. Chen, N. Ren, B. Li, Y. Y. Wu, G. O. Rankin, Y. Rojanasakul, Y. M. Wang and Y. C. Chen, Standardized saponin extract from baiye No.1 tea (camellia sinensis) flowers induced S phase cell cycle arrest and apoptosis via AKT-MDM2-p53 signaling pathway in ovarian cancer cells, *Molecules*, 2020, 25, 3515–3530.
42. F. Caccuri, M. Sommariva, S. Marsico, F. Giordano, A. Zani, A. Giacomini, C. Fraefel, A. Balsari and A. Caruso, Inhibition of DNA repair mechanisms and induction of apoptosis in triple negative breast cancer cells expressing the human herpesvirus 6 U94, *Cancers (Basel).*, 2019, 11, 1006–1025.
43. A. M. Noonan, A. Cousins, D. Anderson, K. P. Zeligs, K. Bunch, L. Hernandez, Y. Shibuya, I. S. Goldlust, R. Guha and M. T. Ferrer, Matrix drug screen identifies synergistic drug combinations to augment SMAC mimetic activity in ovarian cancer, *Cancers (Basel).*, 2020, 12, 3784–3802.
44. L. M. Chen, G. D. Li, F. Peng, X. M. Jie, G. Z. Dongye, K. R. Cai, R. B. Feng, B. J. Li, Q. W. Zeng, K. Y. Lun, J. C. Chen and B. L. Xu, The induction of autophagy against mitochondria-mediated apoptosis in lung cancer cells by a ruthenium(II) imidazole complex, *Oncotarget*, 2016, 7, 80716–80734.
45. S. H. Huang, L. W. Wu, A. C. Huang, C. C. Yu, J. C. Lien, Y. P. Huang, J. S. Yang, J. H. Yang, Y. P. Hsiao, W. G. Wood, C. S. Yu and J. G. J. Agric, Benzyl isothiocyanate (BITC) induces G2/M phase Arrest and apoptosis in human melanoma A375.S2 cells through reactive oxygen species (ROS) and both mitochondria dependent and death receptor-mediated multiple signaling pathways, *Food Chem.*, 2012, 60, 665–675.
46. J. C. Chen, J. Wang, Y. Y. Deng, B. J. Li, L C. P., Y. X. Lin, D. B. Yang, H. Y. Zhang, L. M. Chen and T. Wang, Novel cyclometalated Ru(II) complexes containing isoquinoline ligands: Synthesis, characterization, cellular uptake and in vitro cytotoxicity, *Eur. J. Med. Chem.*, 2020, 203, 112562–112577.
47. C. Lange, C. Lehmann, M. Mahler and P. J. Bednarski, Comparison of cellular death pathways after mTHPC-mediated photodynamic therapy (PDT) in five human cancer cell lines, *Cancers (Basel).*, 2019, 5, 702–733.
48. T. Chen and Y. S. Wong, Selenocystine induces apoptosis of A375 human melanoma cells by activating ROS-mediated mitochondrial pathway and p53 phosphorylation, *Cell Mol. Life Sci.*, 2008, 65, 2763–2775.
49. Z. Zhang, Q. Wu, X. H. Wu, F. Y. Sun, L. M. Chen, J. C. Chen, S. L. Yang and W. J. Mei, Ruthenium(II) complexes as apoptosis inducers by stabilizing c-myc Gquadruplex DNA, *Eur. J. Med. Chem.*, 2014, 80, 316–324.
50. H. Q. Lai, Z. N. Zhao, L. L. Li, W. J. Zheng and T. F. Chen, Antiangiogenic ruthenium(II) benzimidazole complexes, structure-based activation of distinct signaling pathways, *Metallomics*, 2015, 7, 439–447.
51. B. M. Cumming, K. W. Addicott, J. H. Adamson and A. J. Steyn, Mycobacterium tuberculosis induces decelerated bioenergetic metabolism in human macrophages, *Elife*, 2018, 7, e39169.
52. D. N. Das, P. P. Naik, S. Mukhopadhyay, P. K. Panda, N. Sinha, B. R. Meher and S. K. Bhutia, Elimination of dysfunctional mitochondria through mitophagy suppresses benzo[a]pyrene-induced apoptosis, *Free Radical Biol. Med.*, 2017, 112, 452–463.
53. P. Naserzadeh, S. N. Mehr, Z. Sadabadi, E. Seydi, A. Salimi and J. Pourahmad, Curcumin protects mitochondria and cardiomyocytes from oxidative damage and apoptosis induced by hemiscorpius lepturus venom, *Drug. Res.*, 2018, 68, 113–120.
54. H. Hochberg-Laufer, N. Neufeld, Y. Brody, S. Nadav-Eliyahu, R. Ben-Yishay and Y. Shav-Tal, Availability of splicing factors in the nucleoplasm can regulate the release of mRNA from the gene after transcription, *PLoS Genet.*, 2019, 15, e1008459.
55. M. Corvaisier and M. Alvarado-Kristensson, Non-canonical functions of the gamma-tubulin meshwork in the regulation of the nuclear architecture, *Cancers (Basel).*, 2020, 11, 3102–3121.
56. M. Zhang, Q. S. Lu, H. M. Hou, D. Q. Sun, M. J. Chen, F. Ning, P. H. Wu, D. Wei, Y. Y. Duan, Y. Pan and G. E. Lash, Garcinol inhibits the proliferation of endometrial cancer cells by inducing cell cycle arrest, *Oncol. Rep.*, 2021, 45, 630–640.
57. X. J. Liu, M. Y. Song, Z. L. Gao, X. K. Cai, W. Dixon, X. F. Chen, Y. Cao and H. Xiao. J. Agric, Stereoisomers of astaxanthin inhibit human colon cancer cell growth by inducing G2/M Cell cycle arrest and apoptosis, *Food Chem.*, 2016, 64, 7750–7759.
58. Y. Q. Guan, Z. B. Li, A. N. Yang, H. Zheng, Z. Zheng, L. Zhang, L. Li and J. M. Liu, Cell cycle arrest and apoptosis of OVCAR-3 and MCF-7 cells induced by co-immobilized TNF-α plus IFN-γ on polystyrene and the role of p53 activation, *Biomaterials*, 2012, 33, 6162–6171.
59. J. Y. Kim, H. Lee, J. Woo, W. Yue, K. Kim, S. Choi, J. J. Jang, Y. Kim, I. A. Park, D. Han and H. S. Ryu, Reconstruction of pathway modification induced by nicotinamide using multi-omic network analyses in triple negative breast cancer, *Sci. Rep.*, 2017, 7, 3466–3478.
60. J. K. Buolamwini, Cell cycle molecular targets in novel anticancer drug discovery, *Curr. Pharm. Design*, 2000, 6, 379–392.
61. R. M. Golsteyn, Cdk1 and Cdk2 complexes (cyclin dependent kinases) in apoptosis: a role beyond the cell cycle, *Cancer Lett.*, 2005, 217, 129–138.
62. J. Farrés, L. Llacuna, J. Martin-Caballero, C. Martínez, J. J. Lozano, C. Ampurdanés, A. J. López-Contreras, L. Florensa, J. Navarro, E. Ottina, F. Dantzer, V. Schreiber, A. Villunger, O. Fernández-Capetillo and J. Yélamos, PARP-2 sustains erythropoiesis in mice by limiting replicative stress in erythroid progenitors, *Cell Death Differ.*, 2015, 22, 1144–1157.
63. J. S. Park, D. Y. Shin, Y. W. Lee, C. K. Cho, G. Y. Kim, W. J. Kim, H. S. Yoo and Y. H. Choi, Apoptotic and anti-metastatic effects of the whole skin of venenum bufonis in A549 human lung cancer cells, *Int. J. Oncol.*, 2012, 40, 1210–1219.
64. S. Fu, X. Chen, H. W. Lo and J. Lin, Combined bazedoxifene and paclitaxel treatments inhibit cell viability, cell migration, colony formation, and tumor growth and induce apoptosis in breast cancer, *Cancer Lett.*, 2019, 448, 11–19.
65. Y. Wang, D. Chen, H. L. Qian, Y. S. Tsai, S. J. Shao, Q. Liu, D. Dominguez and Z. F. Wang, The splicing factor RBM4 controls apoptosis, proliferation, and migration to suppress tumor progression, *Cancer Cell*, 2014, 26, 374–389.